Influence of Ca-deficiency on the magneto-transport properties in $La_{0.8}Ca_{0.2}MnO_3$ perovskite and estimation of magnetic entropy change

M. Khlifi,[1,a)] M. Bejar,[1] E. Dhahri,[1] P. Lachkar,[2] and E. K. Hlil[3]
[1]*Laboratoire de Physique Appliquée, Faculté des Sciences de Sfax, B.P. 802, Sfax 3018, Tunisie*
[2]*MCBT, Institut Néel, CNRS-25 Avenue des Martyrs, bâtiment E, BP 166, 38042 Grenoble cedex 9, France*
[3]*Institut Néel, CNRS–Université J. Fourier, BP 166, 38042 Grenoble, France*

(Received 15 February 2012; accepted 16 April 2012; published online 21 May 2012)

$La_{0.8}Ca_{0.2-x}\square_xMnO_3$ ($x = 0.00$, 0.10, and 0.20) perovskite was prepared by the conventional solid-state reaction and annealed at 1473 K. X-ray diffraction and scanning electron microscopy shown the existence of a secondary phase attributed to the unreacted Mn_3O_4 oxide. The magneto transport properties have been investigated based on the temperature dependence of the resistivity $\rho(T)$ measurements under several applied magnetic fields. We note that the $La_{0.8}Ca_{0.2}MnO_3$ ($x = 0.00$) sample has a classical metal-insulator transition at T_ρ. But we have observed that the lacunars samples ($x = 0.10$ and 0.20) include a metallic and insulator behavior simultaneously below T_ρ and the resistivity is dominated by tunneling through the barriers associated with the insulating phase. In other words, the calcium deficiency favors the enhancement of the insulator behavior. The electrical resistivity is fitted with the phenomenological percolation model, which is based on the phase segregation of ferromagnetic metallic clusters and paramagnetic insulating regions. Furthermore, we found that the estimated results are in good agreement with experimental data. Above all, the resistivity dependence on the temperature and magnetic field data is used to deduce the magnetic entropy change. We have found that these magnetic entropy change values are similar to those calculated in our previous work from the magnetic measurements. Finally, we have found an excellent estimation of the magnetic entropy change based on the Landau theory.
 [http://dx.doi.org/10.1063/1.4718450]

I. INTRODUCTION

Recently, doped manganites with general formula $Ln_{1-x}A_xMnO_3$ (where Ln is a rare earth: La, Pr, Sm, and A is a divalent element: Ca, Sr, Ba…) have attracted considerable research interest. Numerous studies have been devoted in the rare earth manganite perovskite which are exhibiting colossal magnetoresistance (CMR) properties[1–3] as well as a magnetocaloric effect (MCE).[4–7] These materials have a wide range of technological applications such as read heads for magnetic information storage, spintronic applications, and magnetic refrigeration. For this reason, it is essential to study their electric and magnetic properties.

Experimentally, those manganites exhibit a metal-to-insulator transition accompanied by a ferromagnetic-to-paramagnetic transition near the Curie temperature T_C. The metallic behavior is usually described in terms of electron scattering process and electron–phonon interaction.[8] On the other hand, in the insulator state the carriers are localized as small polarons due to a strong Jahn Teller (JT) distortion. In this state, the electrical conduction is governed by small polaron hopping mechanism.[9–11] In order to understand the electrical behavior in the whole temperature range, Li *et al.*[12] have developed a new model based on the phase segregation mechanism.[13] This model supposes that the materials are composed of paramagnetic and ferromagnetic regions. Going from the metallic phase to insulating phase, ferromagnetic regions become paramagnetic. Following this mechanism, the electrical resistivity at any temperature is determined by the change of the volume fractions of both regions.

Further, the double exchange theory[14–16] qualitatively shows a correlation between ferromagnetism and electrical conductivity in some manganites.[17,18] Also, we can see a strong correlation between resistivity and magnetic entropy change (ΔS_M) described by Xiong *et al.*[19] So we can calculate ΔS_M based on the electric measurement.

In this paper, we have studied the calcium deficiency effect on the resistivity behavior, and we have simulated it based on the representations of the percolation theory. Then we have deduced the magnetic entropy change ($-\Delta S_M$) from resistivity versus temperature under several applied magnetic field. Finally, we found that the deduced ($-\Delta S_M$) values are in agreement with those determined from magnetic measurements and those calculated from the Landau theory.

II. EXPERIMENTAL

The $La_{0.8}Ca_{0.2}MnO_3$ sample was prepared using the conventional solid-state reaction described previously.[20] The sample structure was characterized by x-ray diffraction with CuKα radiation ($\lambda = 1.5406$ Å). Then, the morphologies of products were investigated using a scanning electron microscope (SEM). Electrical measurements were recorded in a "quantum design" physical properties measurement system (PPMS) in a temperature ranging from 2 to 300 K under several magnetic fields rising from 0 to 5 T.

a)Author to whom correspondence should be addressed. Electronic mail: khlifimouadh3000@yahoo.fr.

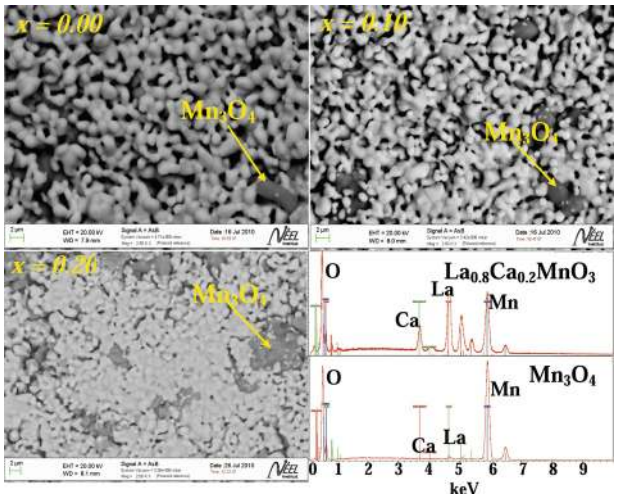

FIG. 1. Scanning electron micrographs of $La_{0.8}Ca_{0.2-x}\square_xMnO_3$ samples ($x=0.00$, $x=0.10$, and $x=0.20$) and the EDX analysis of chemical species of $x=0.00$ sample.

III. RESULTS AND DISCUSSIONS

SEM micrographs are performed using the Angle-selective Backscattered electron (AsB) detector. These Backscattered electrons are sensitive to the atomic number of atoms in the sample, so the areas formed of atoms with high atomic number appear brighter than others. This method will help to measure the chemical homogeneity of a sample and to allow a qualitative analysis. SEM micrographs of all samples given in Fig. 1 show the coexistence of two phases in our samples. The main proportion is attributed to the principal $La_{0.8}Ca_{0.2-x}\square_xMnO_3$ (white) phase; the secondary minor phase is attributed to the unreacted Mn_3O_4 (dark). The presence of two phases is confirmed by the Energy Dispertive X-ray (EDX) analysis of chemical species, where the electron beam is focused on the white area then on the dark one (Fig. 1). This result is illustrated in our previous work[20] using the x-ray diffraction (XRD), when a supplementary peak is superimposed with the Mn_3O_4 Bragg-position. Also, from Fig. 1 we can notice that the Mn_3O_4 quantity percentage increases when x increases. Moreover, the x-ray patterns

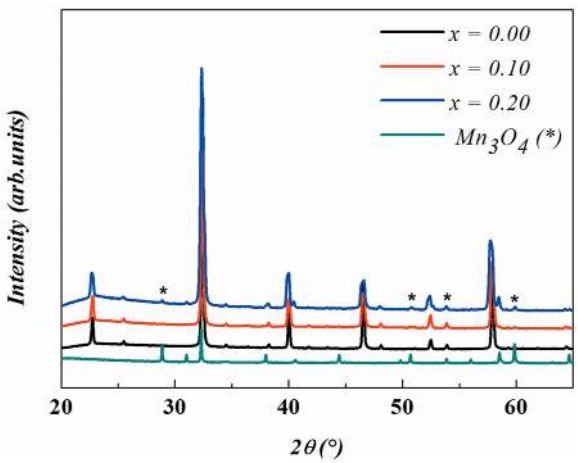

FIG. 2. XRD patterns of $La_{0.8}Ca_{0.2-x}\square_xMnO_3$ and Mn_3O_4 compounds. Asterisk marks the tiny impurity of Mn_3O_4.

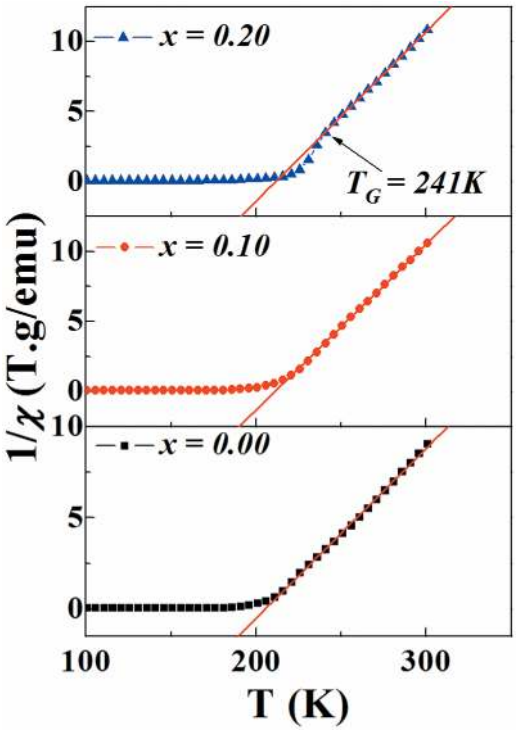

FIG. 3. Inverse of magnetic susceptibility ($1/\chi$) versus temperature (T) for $La_{0.8}Ca_{0.2-x}\square_xMnO_3$ samples ($x=0.00$, $x=0.10$, and $x=0.20$) measured at applied magnetic field of 0.05 T.

(Fig. 2) show that the intensity of Mn_3O_4 peaks increase with the calcium deficiencies. This confirms that the percentage of this secondary phase increases when increasing the calcium deficiency. It is important to note that the stoichiometry of $La_{0.8}Ca_{0.2-x}\square_xMnO_3$ phase is not affected by the formation of Mn_3O_4 secondary phase.[21]

Besides, our curves of magnetization as a function of temperature[20] reveals that all samples exhibit a magnetic transition from the paramagnetic (PM) state to ferromagnetic (FM) one. According to the formula $La^{3+}_{0.8}Ca^{2+}_{0.2-x}\square_xMn^{3+}_{0.8-2x}Mn^{4+}_{0.2+2x}O^{2-}_3$, the increase of x leads to the reduction of double exchange (DE) mechanism between Mn^{3+} and Mn^{4+} ions. This explains the decrease of the magnetization when increasing the calcium deficiency. In Fig. 3, we report the inverse of magnetic susceptibility (χ^{-1}) as a function of temperature. For the samples with $x=0.00$ and $x=0.10$, χ^{-1} follows the Curie-Weiss law (linear behavior in the paramagnetic region). The down turn in the magnetic susceptibility at temperatures above T_C for the sample with $x=0.20$ is the signature of the "Griffiths phase."[22] The deviation from Curie-Weiss law in the PM region is due to the presence of FM clusters within the PM region.

The temperature dependence of electric resistivity plotted in Fig. 4 shows that all samples have a ferromagnetic-metallic to paramagnetic-insulator transition near T_ρ. However, the calcium deficiency leads to increase the values of the resistivity due to the reduction of the DE interaction between spins of Mn^{3+} and Mn^{4+} ions. Below T_ρ, the lacunars samples ($x=0.10$ and 0.20) show a complex electrical behavior characterized by a minimum of resistivity in the metallic state, and then begin to increase when decreasing temperature. This can be explained by a co-existence of metallic and insulator

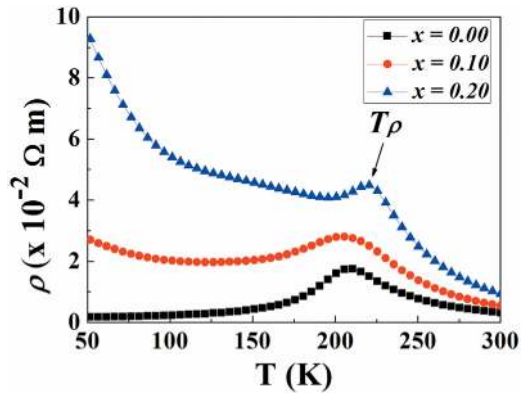

FIG. 4. Zero field electrical resistivity (ρ) as a function of temperature (T) $La_{0.8}Ca_{0.2-x}\square_xMnO_3$ samples ($x = 0.00$, $x = 0.10$, and $x = 0.20$).

behavior. That is due to the fact that the electrical resistivity of our materials depends on the respective volume fractions of the $La_{0.8}Ca_{0.2-x}\square_xMnO_3$ and Mn_3O_4 phases. We know that the pure Mn_3O_4 oxide has a high resistivity values on the order of 10^8 Ω cm at room temperature and higher values for $T < 300$ K.[23] Moreover, at low temperatures, the resistivity is dominated by tunneling through the barriers associated with long intrinsic structural defects, such as grain boundaries and inclusions of the insulating phase.[24–26] In our case, the insulating Mn_3O_4 secondary phase can be considered as energy barriers for the electrical transport process. So, the increase of the resistivity values of the $La_{0.8}Ca_{0.2-x}\square_xMnO_3$ samples with increasing x has been also explained by the increase of the high resistive Mn_3O_4 phase concentration. It is remarkable, on the one side, that T_ρ decreases when the rate deficiency increases between $x = 0.00$ and $x = 0.10$ samples. On the other side, the increase of T_ρ for $x = 0.20$ is due to the onset of Griffiths phase in these samples when the ferromagnetic clusters cause a delay of the metal-insulator transition (Fig. 4).

In order to understand the transport mechanism in our samples, we will use a theoretical model which describes it. Taking $La_{0.8}Ca_{0.2}MnO_3$ ($x = 0.00$) sample into consideration, the resistivity increases when decreasing temperature from 300 K and reaches a maximum at T_ρ. This region ($T > T_\rho$) is characterized by a semiconductor behavior which is described by the adiabatic small polaron hopping mechanism[9–11] according to the following formula:

$$\rho(T) = CT\exp\left(\frac{E_a}{K_BT}\right), \tag{1}$$

where C is a pre-exponential coefficient, E_a is the activation energy, and K_B is the Boltzmann constant. In low-temperature ferromagnetic phase ($T < T_\rho$), the $\rho(T)$ curve is approximated by an expression that includes several scattering mechanisms according to the following formula:

$$\rho(T) = \rho_0 + AT^2 + BT^5, \tag{2}$$

where ρ_0 is the residual resistivity, the AT^2 term is attributed to the single-magnon's scattering contribution, and the BT^5 term is attributed to the electron–phonon interaction.[8] For the lacunars samples ($x = 0.10$ and 0.20), we can use the scattering mechanisms model only for a short range below the metal-insulator transition temperature T_ρ where these materials are characterized by a metallic behavior ($d\rho/dT > 0$).

Unfortunately, the small polaron hopping mechanism and scattering one (Eqs. (1) and (2)) cannot describe the electric behavior near the metallic-insulator temperature T_ρ. In order to understand the transport mechanism in the entire temperature range, Li *et al.*[12] have developed a new phenomenological model based on the phase segregation mechanism (percolation approach).

The percolation approach assumes that the materials are composed of paramagnetic and ferromagnetic regions. The semiconductor-like transport properties are exhibited in the paramagnetic regions, while metallic transports always show up in ferromagnetic regions. Then the electrical resistivity of the system at any temperature is determined by the change of the FM volume fractions in both regions. According to Li *et al.*,[12] the resistivity is formulated as

$$\rho(T) = \rho_{FM}f + \rho_{PM}(1-f), \tag{3}$$

where f and $(1-f)$ are the volume fractions of FM domains and PM regions, respectively. The f function well satisfies the Boltzmann distribution given as

$$f = \frac{1}{1+\exp(\Delta U/K_BT)}, \tag{4}$$

where ΔU is the energy difference between FM and PM state. In this percolation approach, $\Delta U(T)$ can be developed around T_C^{mod} at the first order of $(T - T_C^{mod})$. Therefore, we may write

$\Delta U \approx U_0(1 - T/T_C^{mod})$. In this expression, T_C^{mod} is PI–FM transition temperature used in this model and near/equal to T_C, U_0 is taken as the energy difference for temperature well below T_C^{mod}.[12] So, the total resistivity in whole temperatures ranges can be written as

$$\rho(T) = (1-f)\times CT\exp\left(\frac{E_a}{K_BT}\right) + f\times(\rho_0 + AT^2 + BT^5). \tag{5}$$

Figs. 5(a)–5(c) display the simulated (solid line) and experimental results for the $\rho(T)$ curves obtained at zero-field, 2 T and at 5 T for all samples $x = 0.00$, $x = 0.10$, and $x = 0.20$, respectively. It can be seen that the results calculated from Eq. (5) agree with the experimental data. Then, we found that the percolation model describes well enough the resistivity behavior in a wide temperature ranges including the region of phase transition whatever the external magnetic field. The best-fit parameters are given in Table I.

Fig. 6 shows the ferromagnetic phase volume fraction as a function of temperature $f(T)$ for all samples. It is clear that $f(T)$ remains equal to 1 below the metal-insulator transition temperature. That confirms the strong dominance of FM fraction in this range. Then, FM volume fraction begins to decrease until 0 going from the ferromagnetic-metallic state to the paramagnetic-insulator one. This confirms the validity of the percolation approach which assumes a conversation of ferromagnetic region to paramagnetic one when increasing the temperature.

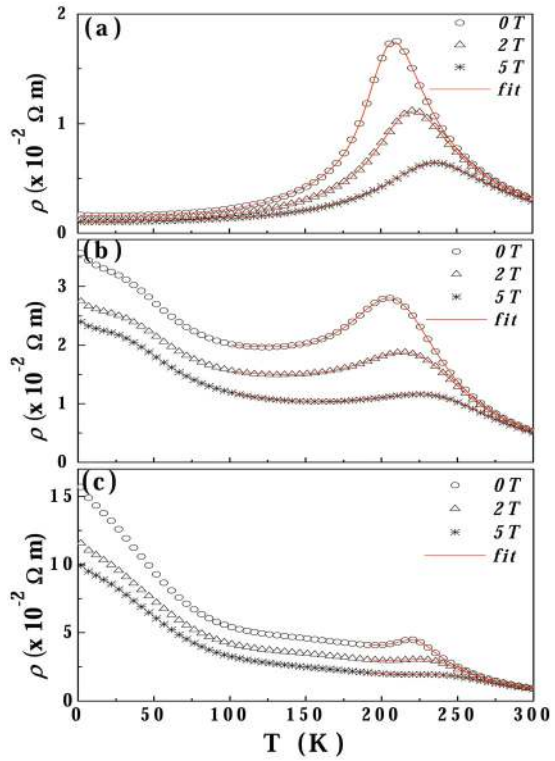

FIG. 5. Electrical resistivity (ρ) as a function of temperature (T) of $La_{0.8}Ca_{0.2-x}\square_xMnO_3$ samples with $x = 0.00$ (*a*), $x = 0.10$, (*b*) and $x = 0.20$ (*c*) under applied magnetic field of 0, 2, and 5 T.

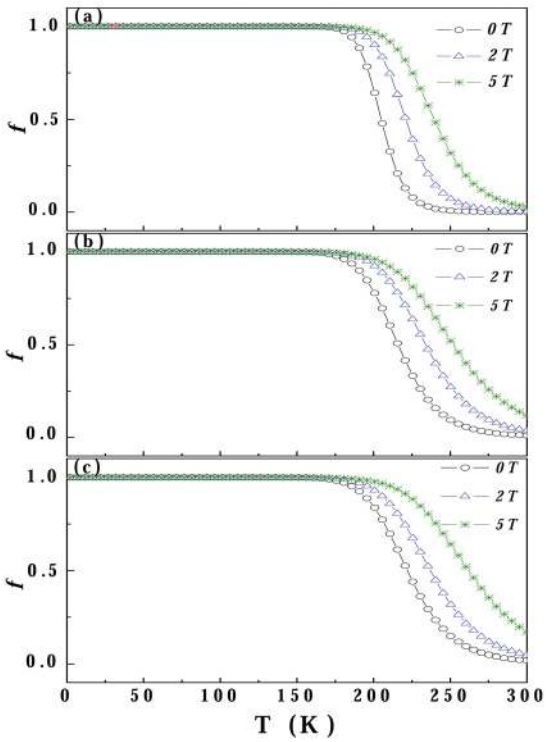

FIG. 6. The temperature dependence of ferromagnetic phase volume fraction for different samples: $x = 0.00$ (*a*), $x = 0.10$ (*b*), and $x = 0.20$ (*c*).

The electrical resistivity of carriers increases when increasing the calcium deficiency rate described above. This is equivalent to the increasing in the activation energy E_a in the transport process of the carriers. Moreover, it can be seen that for all samples the activation energy E_a decreases when increasing the applied magnetic field. Thus, due to the spins' attempt to align along the magnetic field, which favors the conduction and decreases the ability of charge localization and the electrons jumping requires less energy. So the results of E_a are reasonable.

Many researchers have shown a strong correlation between electrical and magnetic properties.[27–29] In manganites, the CMR and MCE effects are usually observed near the magnetic phase transition temperature. It is obvious that there is a relationship between the change in magnetic entropy and resistivity. In this context, Xiong *et al.*[19] proposed a relationship between ΔS_M and ρ given by

$$\Delta S_M = -\alpha \int_0^{\mu_0 H} \left[\frac{\partial Ln(\rho)}{\partial T}\right] d(\mu_0 H), \tag{6}$$

where the parameter α determines the magnetic properties of the sample. For the manganite $La_{0.67}Ca_{0.33}MnO_3$ the parameter α is equal to 21.72 emu/g.[19] For our materials, we found that α is equal to 22.82 emu/g. This is determined from the fitting of ρ versus M curve around the transition temperature T_C with the equation: $\rho = \alpha \exp(-M/T)$[19] (not shown here).

TABLE I. Obtained parameters corresponding to the best fit to the Eq. (5) of the experimental data of $La_{0.8}Ca_{0.2-x}\square_xMnO_3$ samples ($x = 0.00$, 0.10, and 0.20) at 0, 2, and 5 T.

x	ρ_0(Ωm)	$A \times 10^{-8}$ (Ωm/K^2)	$B \times 10^{-14}$ (Ωm/K^5)	$C \times 10^{-8}$ (Ωm)	E_a/K_B (K)	$\Delta U/K_B$ (K)	T_C^{mod} (K)
$x = 0.00$							
0 T	0.0016	3.894	2.279	6.422	1282	5483	206
2 T	0.0012	3.130	1.211	8.061	1233	4792	221
5 T	0.0010	2.838	0.556	13.76	1175	4188	239
$x = 0.10$							
0 T	0.0185	6.321	858.5	5.803	1353	3655	214
2 T	0.0131	11.80	1.053	8.403	1307	3533	230
5 T	0.0118	9.405	93.93	18.59	1287	3513	252
$x = 0.20$							
0 T	0.0601	74.45	3.095	9.614	1385	3432	222
2 T	0.0465	59.40	2.072	13.19	1376	3414	237
5 T	0.0379	67.67	2.931	68.90	1388	3281	262

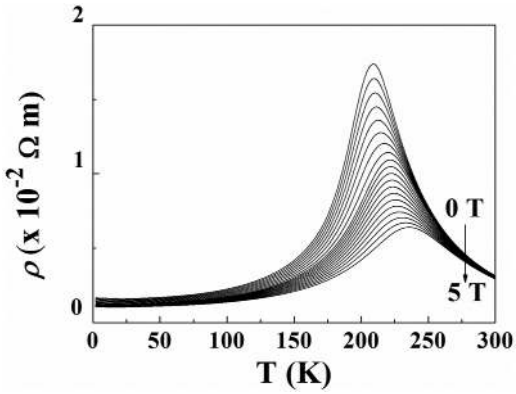

FIG. 7. Temperature dependence of the resistivity under different applied magnetic fields rising from 0 to 5 T for $La_{0.8}Ca_{0.2}MnO_3$ sample ($x = 0.00$).

Now, from the $\rho(H,T)$ curves plotted in Fig. 7, we have estimated the magnetic entropy change (ΔS_M) using Eq. (6), for an applied magnetic field of 5 T. In Fig. 8, we have represented the temperature dependence of magnetic entropy change deduced from the experimental $M(T, \mu_0 H)$ curves, as described in our previous work,[20] and the one calculated from electrical measurement using Eq. (6). We found that the estimated values agree with the experimental ones in the temperature range around T_C. The little difference between these two curves can be explained by the effect of the Mn_3O_4 secondary phase on the electrical properties.

Finally, we have attempted to explain the magnetic entropy change obtained from experimental data based on Landau theory of phase transitions.[30] Very often, Landau's theory of second order phase transition and mean-field approximation is used to describe the magnetic properties. The Gibb's free energy can be written as

$$G(M,T) = G_0 + \frac{a(T)}{2}M^2 + \frac{b(T)}{4}M^4 + \frac{c(T)}{6}M^6 + \ldots - \mu_0 HM, \tag{7}$$

where $a(T)$, $b(T)$, and $c(T)$ are a temperature dependent parameters containing the information of magnetoelastic coupling and electron–electron interaction.[31] From energy minimization, the magnetic equation of state is derived within this theory,

$$\mu_0 H = a(T)M + b(T)M^3 + c(T)M^5. \tag{8}$$

The values of the $a(T)$, $b(T)$, and $c(T)$ parameters and their dependence on temperature can be obtained from experimental isothermal magnetization measurements from polynomial fit of the magnetization (M) versus the applied magnetic field ($\mu_0 H$).

The magnetic entropy is obtained from differentiation of the magnetic part of the free energy with respect to temperature,

$$-S_M(T,\mu_0 H) = \left(\frac{\partial G}{\partial T}\right)_{\mu_0 H} = \frac{a'(T)}{2}M^2 + \frac{b'(T)}{4}M^4 + \frac{c'(T)}{6}M^6. \tag{9}$$

Using the $a(T)$, $b(T)$, and $c(T)$ parameters, the temperature dependence of the magnetic entropy change ($-\Delta S_M$) is calculated through Eq. (9) as shown in Fig. 8. A clear correspondence is found between the experimental magnetic entropy change ($-\Delta S_M$) and the estimated one using Landau theory.

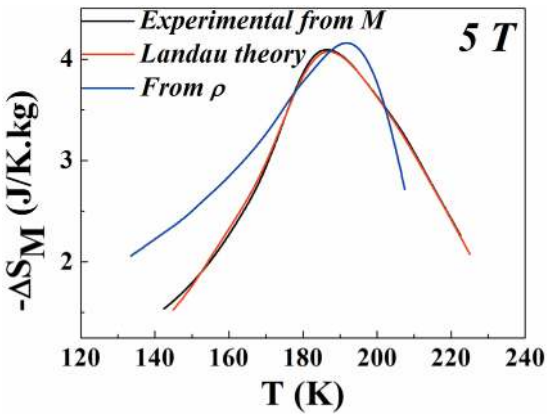

FIG. 8. Temperature dependence of the magnetic-entropy change ($-\Delta S_M$) measured from magnetic, electric measurements and estimated by the Landau theory for an applied magnetic field of 5 T.

IV. CONCLUSION

Electrical properties of $La_{0.8}Ca_{0.2}MnO_3$ compound have been investigated. The temperature dependence of resistivity has revealed the presence of a metal-insulator transition at T_ρ. The conduction mechanism was explained by a small polaron hopping in the insulating region, and by electron scattering mechanisms in the metallic region. Then, to understand the transport mechanism in the entire temperature range, we have used the phenomenological percolation model, which is based on the phase segregation of ferromagnetic metallic clusters and paramagnetic insulating regions.

In addition, from the temperature dependence of the resistivity measured at several applied magnetic field $\rho(H,T)$, we have calculated the magnetic entropy change based on the following equation: $\Delta S_M = -\alpha \int_0^{\mu_0 H} \left[\frac{\partial Ln(\rho)}{\partial T}\right] d(\mu_0 H)$.

The calculated ($-\Delta S_M$) values were found to present a similar maximum of the magnetic entropy change ($-\Delta S_{Max} = 4.15$ J/K kg) to this deduced from the experimental $M(T, \mu_0 H)$ curves, around the Curie temperature T_C. In addition, using the Landau theory, we have found an agreement between the experimental and calculated magnetic entropy change.

[1]V. Shelke, S. Khatarkar, R. Yadav, A. Anshul, and R. K. Singh, J. Magn. Magn. Mater. **322**, 1224 (2010).
[2]L. Li and K. Nishimura, J. Phys.: Conf. Ser. **150**, 042112 (2009).
[3]X. Liu, X. Xu, and Y. Zhang, Phys. Rev. B **62**, 15112 (2000).
[4]Y. Xu, M. Meier, P. Das, M. R. Koblischka, and U. Hartmann, Cryst. Eng. **5**, 383 (2002).
[5]C. B. Zimm, A. Jastrab, A. Sternberg, V. K. Pecharsky, K. A. Gschneidner, Jr., M. Osborne, and I. Anderson, Adv. Cryog. Eng. **43**, 1759 (1998).
[6]K. A. Gschneidner, Jr., V. K. Pecharsky, and A. O. Tsokol, Rep. Prog. Phys. **68**, 1479 (2005).
[7]M. H. Phan and S. C. Yu, J. Magn. Magn. Mater. **306**, 325 (2007).

[8]M. Pękała, V. Drozd, J. F. Fagnard, Ph. Vanderbemden, and M. Ausloos, J. Appl. Phys. **105**, 013923 (2009).
[9]A. de Andres, M. Garcia–Hernandez, J. L. Martinez, and C. Prieto, Appl. Phys. Lett. **74**, 3884 (1999).
[10]M. Ziese and C. Srinitiwarawong, Phys. Rev. B **58**, 11519 (1998).
[11]D. Varshney, D. Choudhary, and M. W. Shaikh, Comput. Mater. Sci. **47**, 839 (2010).
[12]G. Li, H.-D. Zhou, S. L. Feng, X.-J. Fan, and X. G. Li, J. Appl. Phys. **92**, 1406 (2002).
[13]E. Dagotto, T. Hotta, and A. Moreo, Phys. Rep. **344**, 1 (2001).
[14]C. Zener, Phys. Rev. **82**, 403 (1951).
[15]P. W. Anderson and H. Hasegawa, Phys. Rev. **100**, 675 (1955).
[16]P. G. de Gennes, Phys. Rev. **118**, 141 (1960).
[17]A. G. Gamzatov, A. B. Batdalov, and I. K. Kamilov, Physica B **406**, 2231 (2011).
[18]A. G. Gamzatov and A. B. Batdalov, Physica B **406**, 1902 (2011).
[19]C. M. Xiong, J. R. Sun, Y. F. Chen, B. G. Shen, J. Du, and Y. X. Li, IEEE Trans. Magn. **41**, 122 (2005).
[20]M. Khlifi, M. Bejar, O. EL Sadek, E. Dhahri, M. A. Ahmed, and E. K. Hlil, J. Alloys Compd. **509**, 7410 (2011).
[21]B. Vertruyen, J.-F. Fagnard, Ph. Vanderbemden, M. Ausloos, A. Rulmont, and R. Cloots, J. Eur. Ceram. Soc. **27**, 3923 (2007).
[22]M. B. Salamon, P. Lin, and S. H. Chun, Phys. Rev. Lett. **88**, 197203 (2002).
[23]B. Vertruyen, R. Cloots, M. Ausloos, J.-F. Fagnard, and Ph. Vanderbemden, Phys. Rev. B **75**, 165112 (2007).
[24]M. Belogolovskii, G. Jung, V. Markovich, B. Dolgin, X. D. Wu, and Y. Yuzhelevski, J. Appl. Phys. **109**, 073920 (2011).
[25]D. A. Shulyatev and Ya. M. Mukovskii, Phys. Rev. B **64**, 224428 (2001).
[26]G. Jung, V. Markovich, Y. Yuzhelevski, M. Indenbom, C. J. van der Beek, D. Mogilyansky, and Ya. M. Mukovskii, J. Magn. Magn. Mater. **272–276**, 1800–1801 (2004).
[27]M. F. Hundley, M. Hawley, R. H. Heffner, Q. X. Jia, J. J. Neumeier, J. Tesmer, J. D. Thompson, and X. D. Wu, Appl. Phys. Lett. **67**, 860 (1995).
[28]J. O'Donnell, M. Onellion, M. S. Rzchowski, J. N. Eckstein, and I. Bozovic, Phys. Rev. B **54**, 6841 (1996).
[29]B. Chen, C. Uher, D. T. Orelli, J. V. Mantese, A. M. Mance, and A. L. Micheli, Phys. Rev. B **53**, 5094 (1995).
[30]L. D. Landau and E. M. Lifshitz, *Statistical Physics* (Pergamon, New York, 1958).
[31]V. S. Amaral and J. S. Amaral, J. Magn. Magn. Mater. **272–276**, 2104 (2004).